NASA Technical Memorandum 104378

IN-39

40361

P.17

Computational Simulation of High Temperature Metal Matrix Composite Behavior

P.L.N. Murthy and C.C. Chamis
Lewis Research Center
Cleveland, Ohio

NASA
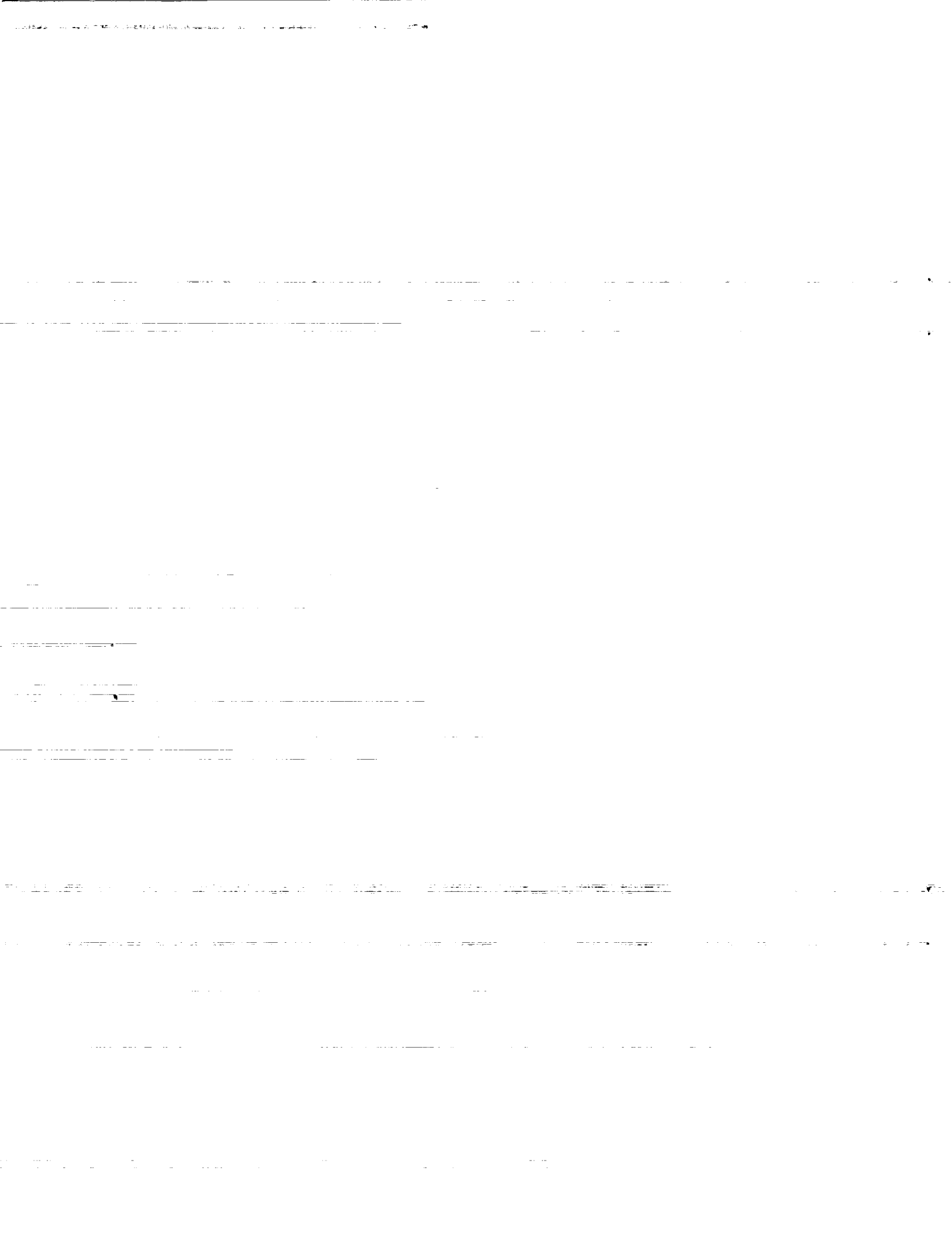
COMPUTATIONAL SIMULATION OF HIGH TEMPERATURE METAL MATRIX COMPOSITE BEHAVIOR

P.L.N. Murthy and C.C. Chamis
National Aeronautics and Space Administration
Lewis Research Center
Cleveland, Ohio 44135

ABSTRACT

Computational procedures are described to simulate the thermal and mechanical behavior of high temperature metal matrix composite (HT-MMC) in the following four broad areas: (1) Behavior of HT-MMC from micromechanics to laminate, (2) HT-MMC structural response for simple and complex structural components, (3) HT-MMC microfracture, and (4) tailoring of HT-MMC behavior for optimum specific performance. Representative results from each area are presented to illustrate the effectiveness of the computational simulation procedures. Relevant reports are referenced for extended discussion regarding the specific area.

INTRODUCTION

Prediction of high temperature metal matrix composite behavior involves analyses at multiple levels due to several inherent scales. These analyses must be integrated progressively from constituent level (fiber and matrix) to the global structural component. The various scales include micromechanics (intraply), macromechanics (interply), laminate (several plies), local region (one finite element) and structural component (assemblage of many finite elements). Obviously, this makes the task very complicated. One approach is to solve the fundamental governing field equations for all the participating variables by using the aid of a computer as an integral part of the solution. Since this approach can be used to simulate the behavior or process as well as a specific event, it is called "Computational Simulation." Computational simulation has been successfully applied at Lewis Research Center to predict the behavior of polymer matrix composites and polymer matrix composite structures. Recently this approach has been extended to simulate the behavior of high temperature metal matrix composites (HT-MMC) and the structural components made therefrom. The objective of the present paper is to briefly describe the computational simulation procedures developed in the following areas: (1) HT-MMC behavior from micromechanics to laminate, (2) HT-MMC structural response for simple and complex structural components, (3) HT-MMC microfracture, and (4) tailored fabrication process for HT-MMC. Representative results from each area are presented to illustrate the effectiveness of the computational simulation. Relevant reports are referenced for extended discussion regarding the specific area.

Behavior of HT-MMC from Micromechanics to Laminate

The behavior of high temperature metal matrix composites from micromechanics to laminate is computationally simulated using the in-house computer code METCAN (METal Matrix Composite ANalyzer). The structure of METCAN, its simulation capabilities, and typical results to illustrate the applications of these capabilities, are summarized in this section.

The structure of METCAN parallels the fabrication process of metal matrix composites. The simulation capability in METCAN is depicted schematically in

figure 1. METCAN has the capability to predict all aspects of HT-MMC behavior, including the fabrication process by using only room temperature properties for the fiber and matrix. The formalism embedded in it, an initial version, and concepts are demonstrated in reference 1. A detailed description of the micromechanics to represent the simulation at the constituent material level is provided in reference 2.

Fundamental to the computational simulation in METCAN is the introduction of the multifactor interaction model (MFIM) to represent the various nonlinearities and their mutual interactions in the constituents. The equation form of the MFIM and the reasons for its selection are summarized in figure 2. A discussion of its ability to represent constituent material behavior and the subsequent influence of this behavior on the response of structural components made from HT-MMC is presented in reference 3.

Verification/validation of the capabilities of METCAN with both experimental results and three-dimensional finite element analysis predictions has been an ongoing in-house activity. References 4 to 6 give the details of these efforts. Illustrative results from reference 6 are shown in figures 3 and 4. METCAN predictions for transverse strengths of SiC/Ti-6-4 at three different temperatures (73 °F, 600 °F, and 800 °F) for a fiber volume ratio of 0.34 are shown in figure 3. Difference between METCAN predictions and experimental results are minimal and the observed experimental degradation in strengths with increasing temperature is accurately predicted by METCAN. Examination of the room temperature stress-strain behavior (fig. 4) shows an almost exact match between METCAN and experiment. The properties used for the constituents as well as the details of the simulation are given in reference 6.

HT-MMC Structural Analysis (HITCAN)

HITCAN (ref. 7) is a general purpose computer code for predicting global structural and local stress-strain response of arbitrarily oriented, multilayered high temperature metal matrix composite structures, both at the constituent (fiber, matrix, and interphase) and the structural level. It combines METCAN with a finite element code, MHOST (ref. 8), and a dedicated mesh generator adapted from COBSTRAN (ref. 9). The code is stand-alone and stream-lined for the thermal/structural analysis of hot metal matrix composite structures. A schematic of the code's structure is shown in figure 5, with its capabilities summarized in table I. An extensive description of HITCAN including a variety of sample cases to illustrate its computational capabilities, can be found in reference 7. The results for a simply supported plate under bending and uniform temperature loading conditions are included herein as specific examples.

The plate geometry, laminate lay-up, and loading conditions (thermal, mechanical) are shown in figure 6. The buckling evaluation results are shown in figure 7. The buckling load decreases with fiber degradation (fiber diffusion into the matrix) and with temperature (material stiffness degrades due to temperature). The decrease, due to temperature, is substantial (about 30 percent). The plate vibration frequencies, displacement, and ply and constituent stresses are summarized in figure 8. The figure illustrates the versatility (breadth and depth) of HITCAN to simulate MMC structural behavior and evaluate their adequacy in hot structures applications. HITCAN can also be used to perform sensitivity analyses. Results from sensitivity analyses for the plate are shown in figure 9. They show the effects of fiber degra-

dation, ply orientation, fabrication process, and material behavior model on the plate response (deflection at the center and stresses at the center).

Collectively, the results summarized demonstrate that the complex behavior of HT-MMC structures can be simulated at all its scales by using an integrated computer code such as HITCAN.

HT-MMC Microfracture

Computational simulation of fiber/matrix fracture and fiber-matrix interface debonding in HT-MMC is part of an ongoing research activity to develop methods for microfracture, microfracture propagation and global fracture toughness of metal matrix composites. Recent efforts (ref. 10), include three-dimensional finite element simulations, which are used to evaluate the effects of partial debonding on unidirectional composite (ply) properties. An extension of this work with emphasis on microfracture, fracture propagation and stress redistribution in surrounding matrix/fibers due to brittle fracture of the fiber/matrix or debonding of the fiber-matrix interface can be found in reference 11. Results from this report for the strain energy release rate under longitudinal and transverse loading are included herein as specific examples.

The finite element model used in this computational simulation procedure consists of a group of nine fibers, all unidirectional, in a three by three unit cell array ("nine cell model"). The modeling details are shown in figure 10. The procedure is illustrated by using a composite system consisting of 35 percent fiber by volume SiC/Ti15 metal matrix composite with the properties as shown in table II. MSC/NASTRAN (ref. 12) is used for the three-dimensional finite element analysis.

The computational details for a typical set of simulations consisted of fracture initiation in the fiber/matrix or at the fiber-matrix interface in the center cell. Fracture is simulated by placing duplicate node points on either side of the crack. Cracks are introduced symmetrically around the center fiber. For a given fracture configuration, fixed boundary displacements are applied to the model in a given direction. Resulting nodal forces corresponding to those applied displacements are found by the finite element analysis. Comparison of resulting nodal forces is made for reduction in global stiffness as the fracture propagates. The corresponding strain energy release rates are computed by using the global approach in which the applied nodal displacements and the corresponding nodal forces obtained from finite element analysis at the loaded end of the composite are used to calculate the work done followed by the strain energy release rate. Global fracture toughness is assumed to be defined by the onset of rapidly increasing strain energy release rate with relatively small increases in fracture propagation.

For the case of longitudinal loading, the strain energy release rate versus the fiber length debonded is shown in figure 11(a) and (b). If the fracture initiates and propagates along the fiber matrix interface, there is no reduction in the global longitudinal stiffness, and the strain energy release rate is also zero. Even though, it requires less energy to drive the crack in the debonding mode, one could not reach this state prior to fiber or matrix fracture. Hence the interface debonding will only occur if it is preceeded by fiber or matrix fracture. It will not initiate by itself. Also, it demonstrates that interface debonding is a weaker fracture mode and is most likely to instantaneously follow the stronger fracture modes (fiber/matrix fracture), when the composite is subjected to longitudinal (along the fiber) loading. The results for the strain energy release rate under transverse

3

loading versus the percentage of fiber surface area debonded are shown in figure 12. The crack growth in this mode is stable. Once, 10 percent of the total fiber surface area is debonded, it takes much less energy to drive the crack further, indicating crack propagation instability and high sensitivity of debonding extension due to transverse loading. Hence, it can be concluded that the transverse tensile test is much more indicative of interfacial conditions than it is of either fiber or matrix conditions.

Collectively the above results demonstrate that microfracture in metal matrix composites can be computationally simulated. Furthermore, by means of global strain energy release rate computations one can establish the hierarchy of probable fracture paths following the initiation of fracture in matrix or fiber or interface.

Tailoring of HT-MMC Fabrication Process

A crucial problem limiting the use of many HT-MMCs is the high residual thermal microstresses developed during the fabrication process. These are due to the large temperature differential and the mismatch between the thermal expansion coefficients of the fiber and matrix. The presence of residual microstresses typically degrades the mechanical performance of the composite and is primarily responsible for the reported poor thermo-mechanical fatigue endurance of many HT-MMCs. It is desirable, therefore, to explore possible ways to reduce, or alternatively control, the development of residual microstresses. One possibility is to use a suitable fiber coating as an interphase layer between the fibers and the matrix to reduce the effects of the fiber/matrix CTE (Coefficient of Thermal Expansion) mismatch (ref. 13). Also, it is possible to obtain reductions in residual stresses by tailoring the combinations of both temperature and consolidation pressure during fabrication (reference 13). Further work along these lines has focused on the systematic development of a concurrent tailoring methodology for the optimal combination of the interphase layer, its properties, and the fabrication process variables. The details of this work can be found in reference 14. A computer code MMLT (Metal Matrix Laminate Tailoring) which includes the above mentioned methodology is under development. This code couples METCAN with an optimizer. Representative results from this work are reported herein to show the concept and usefulness of the methodology in achieving higher performance from HT-MMCs.

The material used for demonstrating the methodology is P100 graphite fiber in copper matrix. Representative properties for the constituents are given in table III. The cool down phase of the fabrication process history is tailored to minimize the resulting residual stresses in the matrix during cool-down from consolidation to room temperature. Constraints (conditions) were imposed in the tailoring procedure so that the residual stresses will not exceed the corresponding matrix strength during cool-down. Figure 13 shows the current and the tailored fabrication processes, Case 1 (the fabrication process optimized alone) and Case 2 (concurrent optimization of the fabrication process and interphase properties), for P100/copper. Both optimized processes follow similar patterns during the cool-down phase. The corresponding residual stress buildups $\left(\sigma_{m11}^A, \sigma_{m22}^A \right)$ in matrix region A (fig. 2.) are shown in figure 14. Both cases show significant reductions in microstresses. The optimum interphase properties are given in table IV. As seen in table IV, all interphase properties increased during the optimization. However, the CTE appears to be the most critical interphase property showing the greatest

4

increase of all the properties. These results demonstrate that the concurrent tailoring methodology can be used to process HT-MMCs for desired matrix stress magnitudes during the fabrication process. As a by product, the sensitivities of the various parameters that influence the optimum fabrication process can be established. For example, in the present study, it appears that the consolidation pressure history and the interphase CTE are the more important parameters that influence the optimum fabrication process.

CONCLUSIONS

Four research activities pertaining to computational simulation aspects of high temperature metal matrix composites (HT-MMC) are described. These activities have resulted in computer codes which can be used to simulate the complex behavior of hot structures made from HT-MMCs. Results from each code for select sample cases are included to illustrate the capabilities of each code. The results from METCAN are for the prediction of room and high temperature strengths of a SiC/Ti-6-4 composite. The results from HITCAN are for a laminated plate subjected to thermal and mechanical loads and including various nonlinearities. The results from the MMC microfrature studies are for the strain energy release rates due to fiber-fracture/matrix-crack under both longitudinal and transverse loads. The results from the concurrent tailoring methodology are for the optimum fabrication cool-down process as well as the interphase properties to achieve minimal thermal residual stresses in a P100/Copper MMC system. Collectively, the results from these sample cases demonstrate that computational simulation methods can be developed to effectively simulate the complex behavior of the high temperature metal matrix composites.

REFERENCES

1. Hopkins, D.A.: Nonlinear Analysis of High-Temperature Multilayered Composite Structures - Turbine Blades. NASA TM-83754, 1984.

2. Hopkins, D.A.; and Chamis, C.C.: A Unique Set of Micromechanics Equations for High Temperature Metal Matrix Composites. NASA TM-87154, 1985.

3. Chamis, C.C.; and Hopkins, D.A.: Thermoviscoplastic Nonlinear Constitutive Relationships for Structural Analysis of High Temperature Metal Matrix Composites. NASA TM-87291, 1985.

4. Chamis; C.C.; Murthy, P.L.N.; and Hopkins, D.A.: Computational Simulation of High Temperature Metal Matrix Composites Cyclic Behavior. NASA TM-102115, 1988.

5. Chamis, C.C., et al.: METCAN Verification Status. NASA TM-103119, 1990.

6. Lee, H J.; Murthy, P.L.N.; and Chamis, C.C.: METCAN Updates for High Temperature Composite Behavior: Simulation/Verification. NASA TM-103682, 1991.

7. Singhal, S.N., et al.: Demonstration of Capabilities of High Temperature Composite Analyzer Code HITCAN. NASA TM-102560, 1990.

8. Nakazawa, S.: The MHOST Finite Element Program: 3-D Inelastic Analysis Methods for Hot Section Components. Volume II - User's Manual. NASA CR-182235, 1989.

9. Aiello, R.A.: Composite Blade Structural Analyzer (COBSTRAN), User's Manual. NASA TM-101461, 1989.

10. Caruso, J.J.; Trowbridge, D.; and Chamis, C.C.: Finite Element Applications to Explore the Effects of Partial Bonding on Metal Matrix Composite Properties. AIAA Paper 89-1175, Apr. 1989.

11. Mital, S.K.; Caruso, J.J.; and Chamis, C.C.: Metal Matrix Composites Microfracture: Computational Simulation. NASA TM-103153, 1990.

12. MSC/NASTRAN, Version 64, Vols. I and II, Users Manual. The MacNeal-Schwendler Corporation, Los Angeles, 1982.

13. Ghosn, L.J.; and Lerch, B.A.: Optimum Interface Properties for Metal Matrix Composites. NASA TM-102295, 1989.

14. Saravanos, D.A.; Murthy, P.L.N.; and Morel, M.: 1990, "Optimum Fabrication Process for Unidirectional Metal-Matrix Composites: A Computational Simulation," NASA TM-102559, 1990.

15. Morel, M.; and Saravanos, D.A.: Concurrent Micromechanical Tailoring and Fabrication Process Optimization for Metal-Matrix Composites. NASA TM-103670, 1990.

TABLE I. – HITCAN CAPABILITIES FOR COMPOSITE MATERIALS

Type of analysis	Type of structure				
	Beam	Plate	Ring	Curved panel	Builtup structure
Static	Tested	Tested	Tested	Tested	Tested
Buckling[a]					
Load stepping					
Modal (natural vibration modes)[b]					
Time domain	------	------	------	------	-------
Loading:					
Mechanical	Tested	Tested	Tested	Tested	Tested
Thermal	Tested	Tested	Tested	Tested	Tested
Cyclic	------	------	------	------	------
Impact	------	------	------	------	------
Constitutive models[c]					
P = constant	Tested	Tested	Tested	Tested	Tested
P = f(T) (temperature dependence)					
P = f(σ) (stress dependence)					
P = f($\dot{\sigma}$) (stress rate dependence)					
P = f(t) (time dependence)					
P = f(T,σ,$\dot{\sigma}$) (combination)	------	------	------	------	-------
P = f(T,σ,$\dot{\sigma}$,t) (combined with time)	Tested	Tested	Tested	Tested	Tested
Fiber degradation	------	-----	-----	-----	------
Fabrication induced stresses	Tested	Tested	Tested	Tested	Tested
Ply orientations[d] (arbitrary)	Tested	Tested	Tested	Tested	Tested
	Tested	Tested	Tested	Tested	Tested

[a]Tested one buckling mode.
[b]Tested four vibration modes.
[c]Constitutive model notation: P, material properties; T, temperature; σ, stress; $\dot{\sigma}$, stress rate; t, time.
[d]Tested three ply orientations: unsymmetric (0/+45/90); symmetric (0/45); balanced (0/90).

TABLE II. – PROPERTIES OF CONSTITUTENT MATERIALS OF SiC/Ti15

	SiC fiber	Ti15 matrix	Interface
Modulus, E, mpsi	62.0	12.3	12.3
Poisson's ratio, ν	0.3	0.32	0.32
Shear modulus, G, mpsi	23.8	4.6	4.6
Coefficient of thermal expansion α, ppm/°F	1.8	4.5	4.5

7

TABLE III. - REPRESENTATIVE CONSTITUENT

MECHANICAL PROPERTIES OF P100/COPPER AT

REFERENCE CONDITIONS

P100 Graphite		Copper	
E_{f11}	$= 105.0$ GPa	E_m	$= 122.1$ GPa
E_{f22}	$= 0.90$ GPa		
G_{f12}	$= 1.10$ GPa	G_m	$= 47.0$ GPa
G_{f23}	$= 0.70$ GPa		
ρ_f	$= 2.16$ g/cm^3	ρ_m	$= 8.86$ g/cm^3
ν_{f12}	$= 0.20$ cm/cm	ν_m	$= 0.30$ cm/cm
ν_{f23}	$= 0.25$ cm/cm		
α_{f11}	$= 0.030$ mcm/cm/°C	α_m	$= 0.331$ mcm/cm/°C
α_{f22}	$= 0.190$ mcm/cm/°C		
S_{f11T}	$= 2.242$ GPa	S_{mN}	$= 0.221$ GPa
S_{f11C}	$= 1.380$ GPa		
S_{f22}	$= 0.1725$ GPa		
S_{f12}	$= 0.1725$ GPa	S_{mS}	$= 0.131$ GPa
S_{f12}	$= 0.0862$ GPa		
S_{f23}			

TABLE IV. - INITIAL AND OPTIMIZED INTERPHASE

PROPERTIES FOR P100/COPPER

Initial (matrix)	Optimum
$E_d = 17.7$ Mpsi	$E_d = 18.8$ Mpsi
$\alpha_d = 9.80$ μin./in./°F	$c_d = 15.0$ μin./in./°F
$S_d = 32.0$ ksi	$S_d = 27.0$ ksi
$k_d = 12$ percent	$k_d = 15$ percent
$k_f = 40$ percent	$k_f = 47$ percent
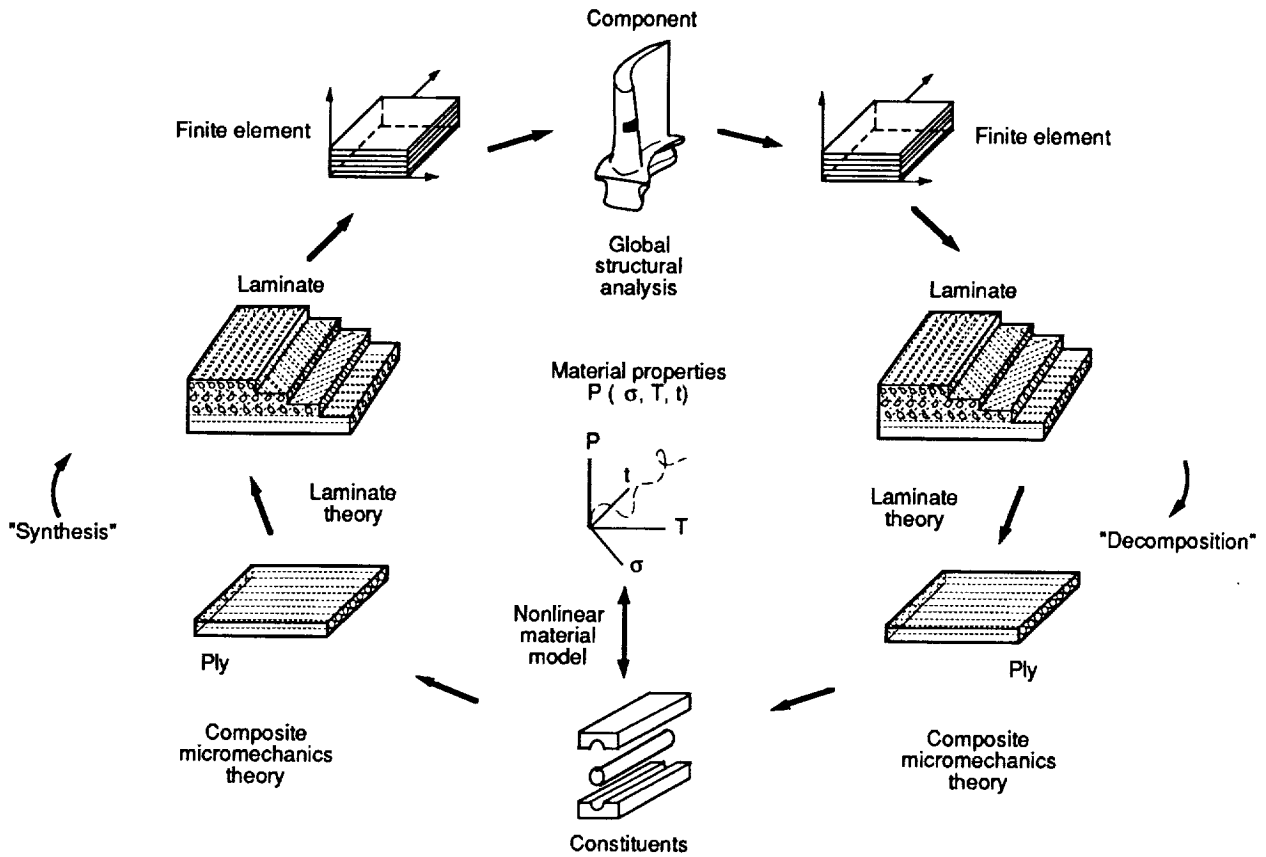
Figure 1.—Integrated approach to metal-matrix composite analysis.

$$\frac{P}{P_O} = \left[\frac{T_F - T}{T_F - T_O}\right]^n \left[\frac{S_F - \sigma}{S_F - \sigma_O}\right]^m \left[\frac{\dot{S}_F - \dot{\sigma}_O}{\dot{S}_F - \dot{\sigma}_O}\right]^l \left[\frac{\dot{T}_F - \dot{T}}{\dot{T}_F - \dot{T}_O}\right]^k \left[\frac{R_F - R}{R_F - R_O}\right]^p L$$

$$L \left[\frac{N_{MF} - N_M}{N_{MF} - N_{MO}}\right]^q \left[\frac{N_{TF} - N_R}{N_{TF} - N_{TO}}\right]^r \left[\frac{t_F - t}{t_F - t_O}\right]^s L$$
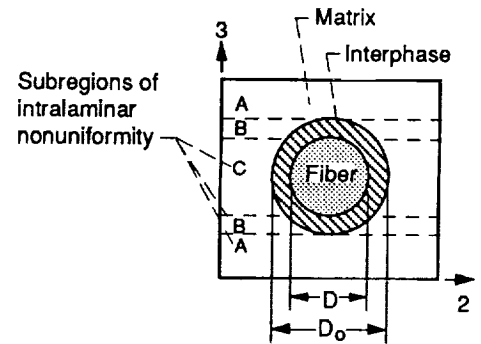
Rationale:

- Gradual effects during most range, rapidly degrading near final stages
- Representative of the in situ behavior for fiber, matrix, interphase, coating
- Introduction of primitive variables (PV)
- Consistent in situ representation of all constituent properties in terms of PV
- Room–temperature values for reference properties
- Continuous interphase growth
- Simultaneous interaction of all primitive variables
- Adaptability to new materials
- Amenable to verification inclusive of all properties
- Readily adaptable to incremental computational simulation

Notations:

P – property; T – temperature; S – strength; R – metallurgical reaction; N – number of cycles:
t – time; over dot – rate; subscripts: O – reference; F – final; M – mechanical; T – thermal

Figure 2.—Assumed multifactor interaction relationship to represent the various factors which influence in situ constituent materials behavior.

9
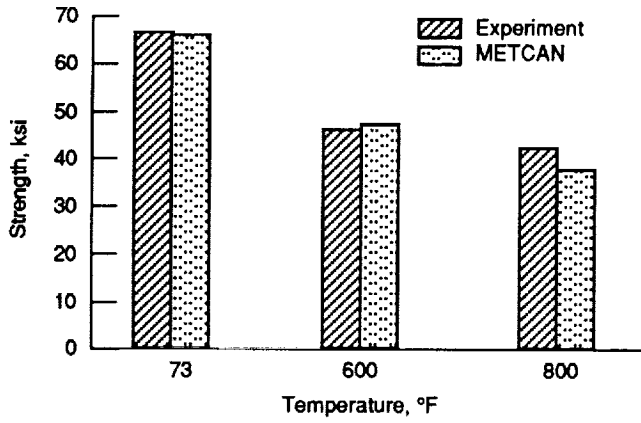
Figure 3.—METCAN predictions of transverse strength of SiC/Ti–6–4; fiber volume ratio, 0.34.
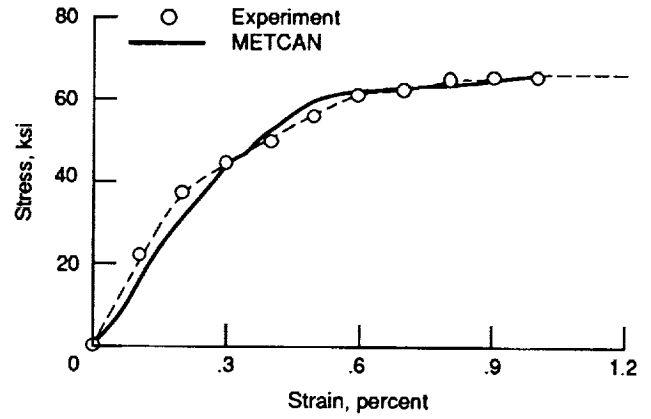
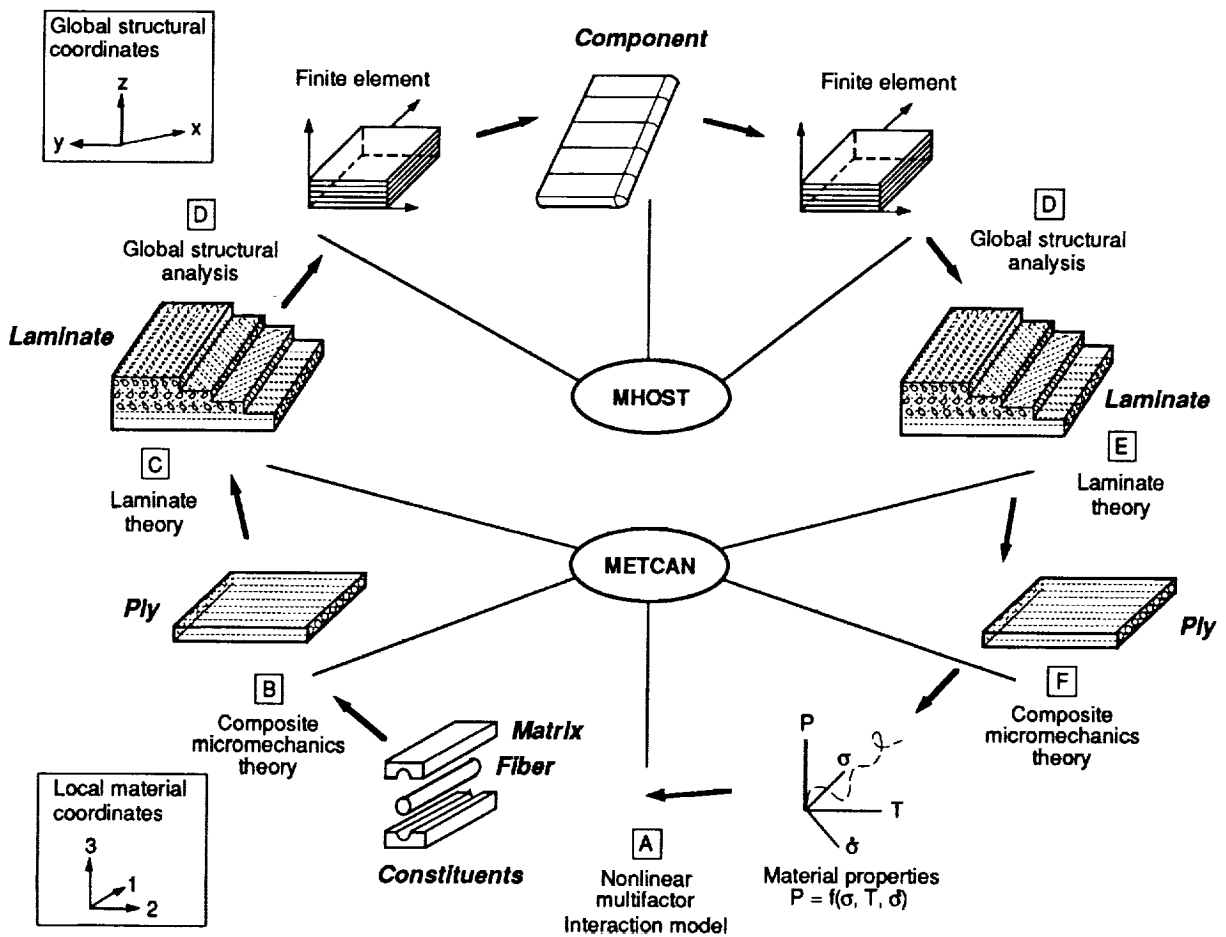Figure 4.—Transverse stress-strain of SiC/Ti–6–4 at 73 °F; fiber volume ratio, 0.34.

Figure 5.—HITCAN: An integrated computer code for high temperature composite structural analysis.

10

Simply supported plate under bending and uniform temperature loadings for (SiC/Ti-15-3-3, 0/±45/90); 0.4 fiber volume ratio
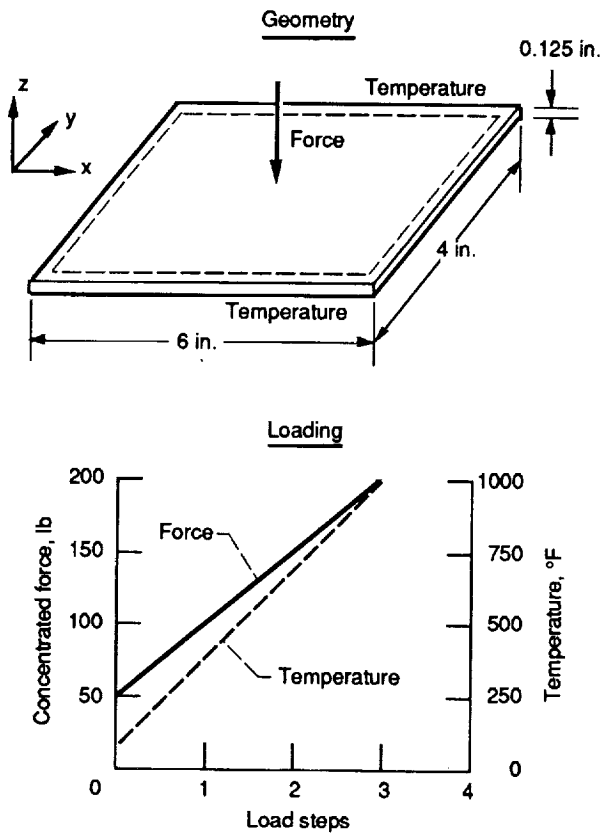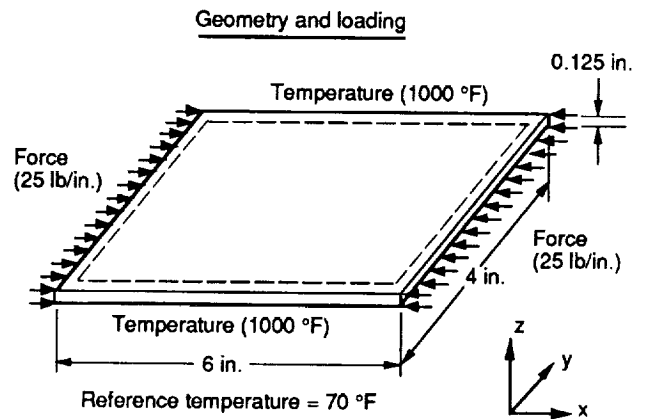
Geometry

Loading

Figure 6.—Geometry and loading for plate.

Simply supported plate under compressive axial and uniform temperature loadings for (SiC/Ti-15-3-3, 0/±45/90); 0.4 fiber volume ratio

Geometry and loading

Reference temperature = 70 °F

Critical buckling force

(i)   Under mechanical loading only = 939 lb/in.
(ii) With fiber degradation, under mechanical loading only = 901 lb/in.
(iii) Under thermo-mechanical loading = 675 lb/in.

Figure 7.—Buckling analysis for plate under thermo-mechanical loading.

Simply supported plate under bending and uniform temperature loadings for (SiC/Ti-15-3-3-3, 0/±45/90); 0.4 fiber volume ratio
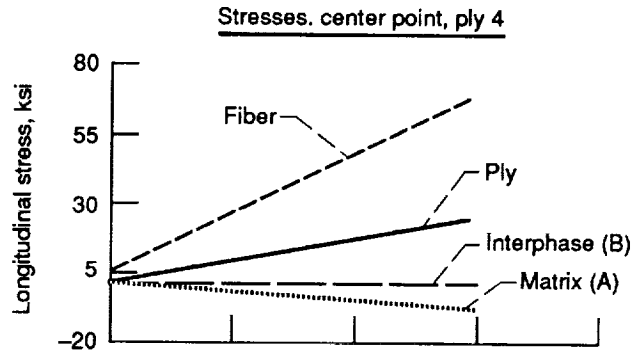
Geometry, boundary conditions, and loading

Natural frequencies

Displacements, center point
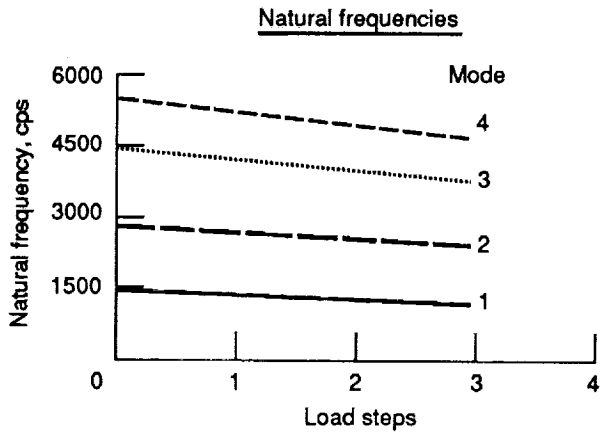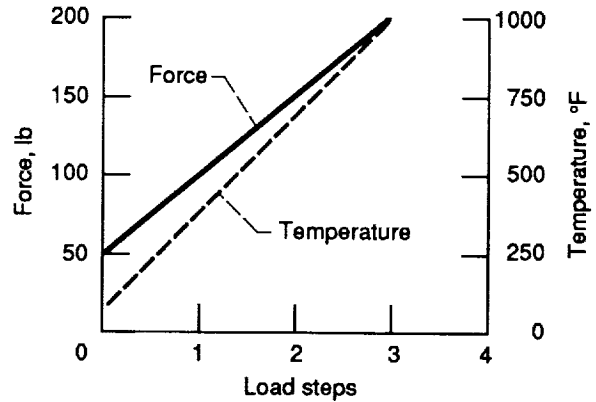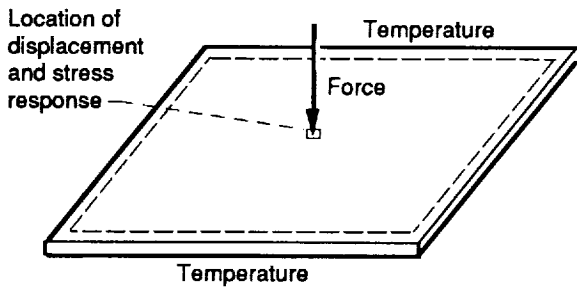

Stresses. center point, ply 4
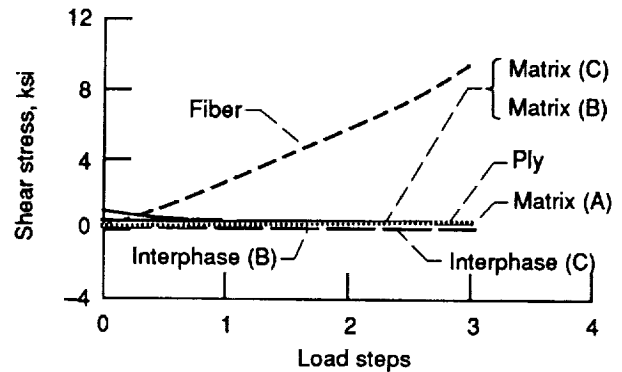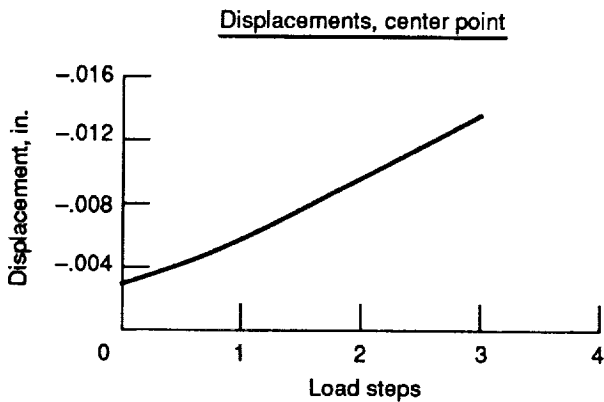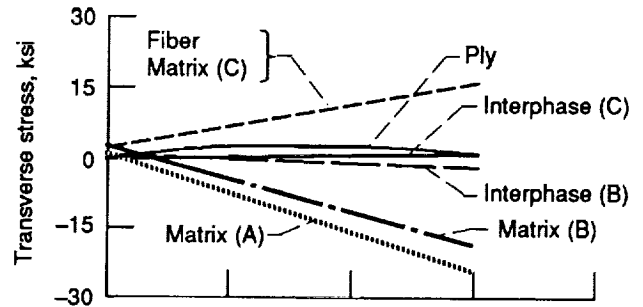
Figure 8.—Base case results for plate.

12

Simply supported plate under bending and uniform temperature loadings for (SiC/Ei-15-3-3, 0/±45/90); 0.4 fiber volume ratio

Response: at load step 3

Effects of

Fiber degradation

Degradation	Disp. (center point), in.	Stresses, Ply 4 (center point), ksi		
		Longitudinal	Transverse	Shear
No	−0.0135	23.9	0.8	1.3
Yes	− .0151	21.8	1.4	1.1

Fabrication-induced stresses

Fabrication-induced stresses	Disp. (center point), in.	Stresses, Ply 4 (center point), ksi		
		Longitudinal	Transverse	Shear
No	−0.0135	23.9	0.8	1.3
Yes	− .0140	18.4	5.8	.4

Ply orientations

Orientation	Disp. (center point), in.	Stresses, Ply 4 (center point), ksi		
		Longitudinal	Transverse	Shear
(0/±45/90)	−0.0135	23.9	0.8	1.3
$(0/45)_s$	− .0144	11.3	7.1	−1.6
$(0/90)_s$	− .0149	13.5	4.7	0

Constitutive relationships
(nonlinear multifactor-interactive model)

Relationship	Disp. (center point), in.	Stresses, Ply 4 (center point), ksi		
		Longitudinal	Transverse	Shear
P = Constant	−0.0119	22.7	2.0	1.1
P = f(T) Temp. dependence	− .0133	25.5	.9	1.3
P = f(σ) Stress dependence	− .0121	21.5	1.9	1.1
P = f($\dot{\sigma}$) Stress rate dependence	− .0118	22.7	2.0	1.1
P = f(T, σ, $\dot{\sigma}$) Combination	− .0135	23.9	.8	1.3

Notation:
P = Material property   T = Temperature
σ = Stress $\dot{\sigma}$ = Stress rate

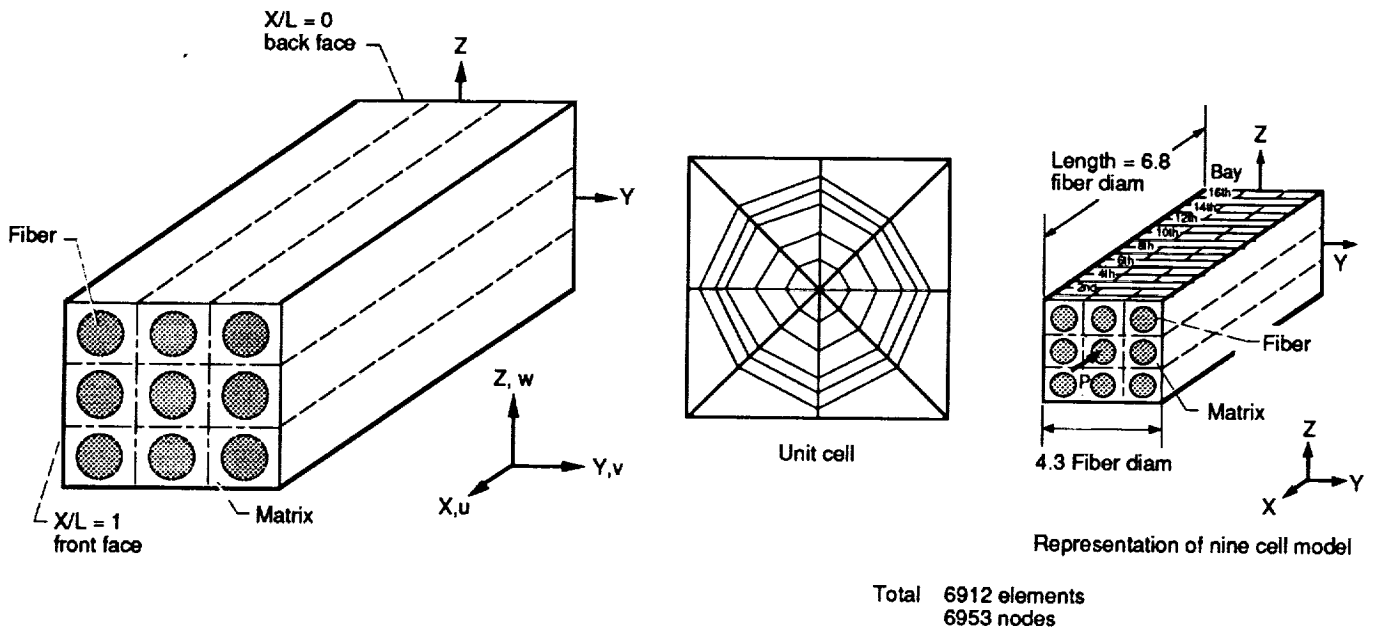Figure 9.—Sensitivity analysis for plate.

13

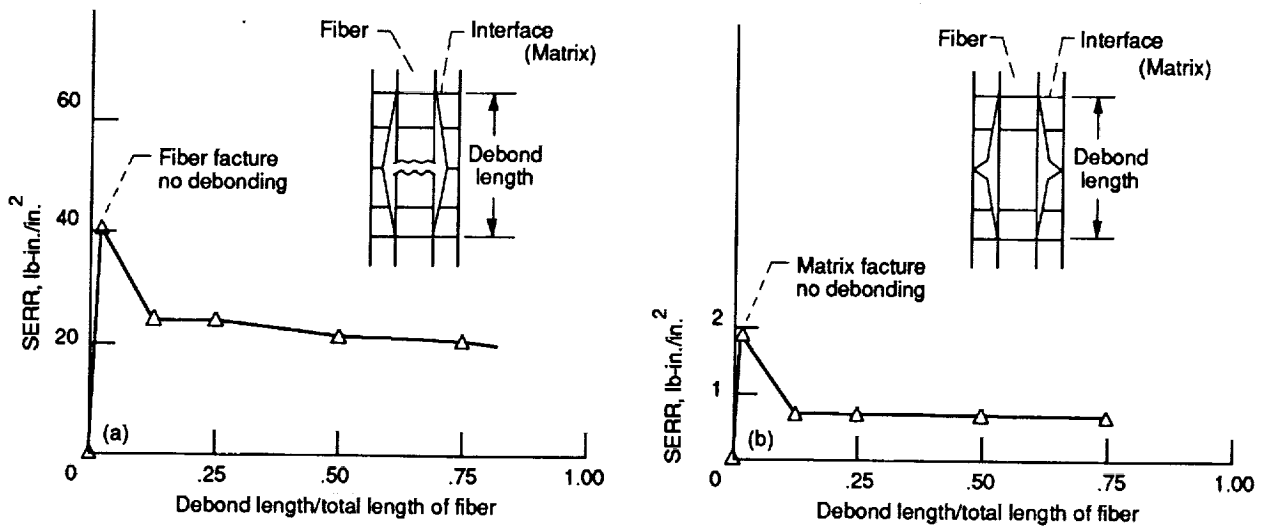Figure 10.—Schematic diagram of nine cell model and finite element details.

Figure 11.—Strain energy release rate for center fiber debonding for longitudinal loading.
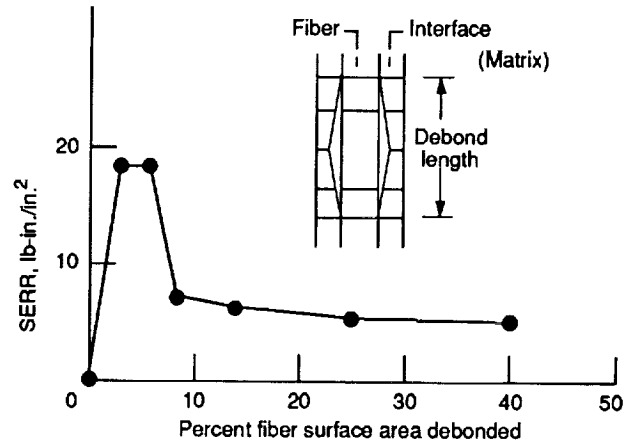
14

Figure 12.—Strain energy release rate vs. percent fiber surface area debonded for transverse loading.
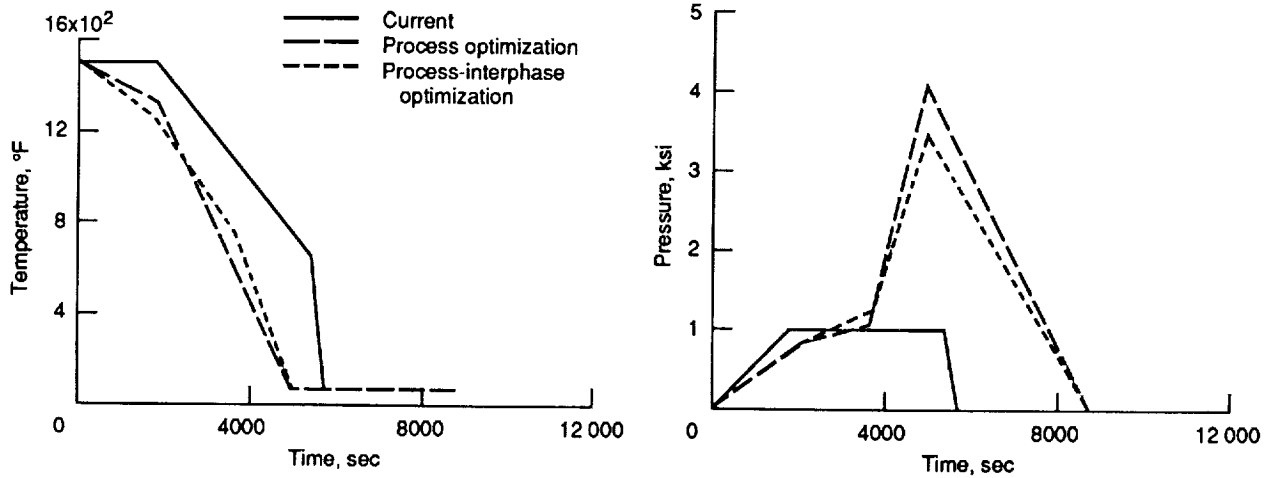

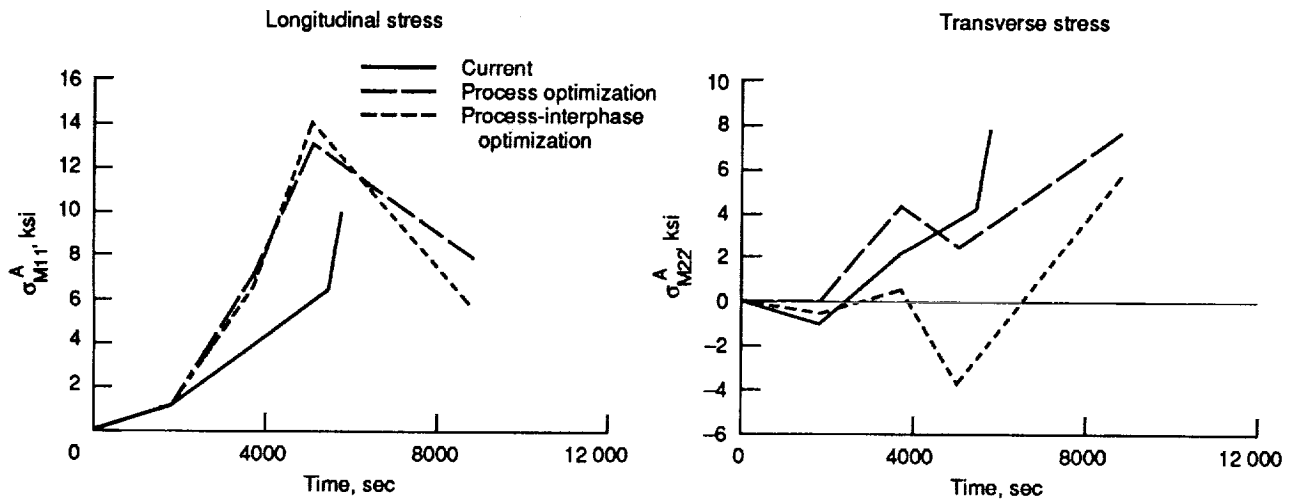Figure 13.—Optimum and current cool-down phases for P100/copper.

Figure 14.—Matrix microstresses developed during the cool-down phase of P100/copper.

16

1. Report No. NASA TM – 104378	2. Government Accession No.	3. Recipient's Catalog No.
4. Title and Subtitle Computational Simulation of High Temperature Metal Matrix Composite Behavior		5. Report Date 6. Performing Organization Code
7. Author(s) P.L.N. Murthy and C.C. Chamis		8. Performing Organization Report No. E – 6183 10. Work Unit No. 510 – 01 – 0A
9. Performing Organization Name and Address National Aeronautics and Space Administration Lewis Research Center Cleveland, Ohio 44135 – 3191		11. Contract or Grant No. 13. Type of Report and Period Covered Technical Memorandum
12. Sponsoring Agency Name and Address National Aeronautics and Space Administration Washington, D.C. 20546 – 0001		14. Sponsoring Agency Code

15. Supplementary Notes

16. Abstract

Computational procedures are described to simulate the thermal and mechanical behavior of high temperature metal matrix composite (HT-MMC) in the following four broad areas: (1) Behavior of HT-MMC from micromechanics to laminate; (2) HT-MMC structural response for simple and complex structural components; (3) HT-MMC micro-fracture; and (4) tailoring of HT-MMC behavior for optimum specific performance. Representative results from each area are presented to illustrate the effectiveness of the computational simulation procedures. Relevant reports are referenced for extended discussion regarding the specific area.

17. Key Words (Suggested by Author(s)) Metal matrix composites; Fabrication; Structural analysis; Mechanical properties; Nonlinearity; Micromechanics; Composite materials; Matrix materials		18. Distribution Statement Unclassified - Unlimited Subject Category 39	
19. Security Classif. (of the report) Unclassified	20. Security Classif. (of this page) Unclassified	21. No. of pages 18	22. Price* A03